LUMINESCENCE PROPERTIES OF $Al_4B_2O_9$:M (M = Dy^{3+}, Sm^{3+}, and Tb^{3+})

İlhan Pekgözlü

Karabük University, Faculty of Engineering, Department of Environmental Engineering, Karabük, Turkey; e-mail: pekgozluilhan@yahoo.com

The objective of this study was to investigate the photoluminescence properties of $Al_4B_2O_9$:M (M = =Dy^{3+}, Sm^{3+}, and Tb^{3+}). The solution combustion method was employed to prepare $Al_4B_2O_9$ doped with M ions. The synthesized aluminum borates were subjected to phase analysis using X-ray diffraction, while their photoluminescence properties were evaluated using a spectrofluorometer. Under excitation at 352 nm, $Al_4B_2O_9$:Dy^{3+} exhibited emission peaks at 484, 578, and 701 nm. Similarly, when excited at 402 nm, $Al_4B_2O_9$:Sm^{3+} emitted light at 563, 599, 645, and 702 nm. Finally, upon excitation at 238 nm, $Al_4B_2O_9$:Tb^{3+} emitted light at 489, 544, 588, and 622 nm.

Keywords: *luminescence, X-ray diffraction, inorganic borate, Rare-earth ions.*

ЛЮМИНЕСЦЕНТНЫЕ СВОЙСТВА АЛЮМОБОРАТОВ $Al_4B_2O_9$:M (M = Dy^{3+}, Sm^{3+}, Tb^{3+})

İ. Pekgözlü

УДК 535.37

Университет Карабюка, Карабюк, Турция; e-mail: pekgozluilhan@yahoo.com

(Поступила 25 ноября 2022)

Исследованы фотолюминесцентные свойства $Al_4B_2O_9$:M (M = Dy^{3+}, Sm^{3+} и Tb^{3+}). Методом сжигания в растворе получен $Al_4B_2O_9$, легированный редкоземельными ионами. Синтезированные бораты алюминия подвергнуты фазовому анализу методом рентгеновской дифракции, а их фотолюминесцентные свойства оценены с помощью спектрофлуориметра. При возбуждении излучением с λ = 352 нм у $Al_4B_2O_9$:Dy^{3+} наблюдались пики эмиссии при 484, 578 и 701 нм. Аналогично при возбуждении излучением с λ = 402 нм $Al_4B_2O_9$:Sm^{3+} излучал свет на λ = 563, 599, 645 и 702 нм. При возбуждении излучением с λ = 238 нм $Al_4B_2O_9$:Tb^{3+} излучал свет с λ = 489, 544, 588 и 622 нм.

Ключевые слова: *люминесценция, рентгеновская дифракция, неорганический борат, редкоземельные ионы.*

Introduction. Rare earth (RE) metals possess intriguing physical and chemical properties, particularly their optical behavior, which has captured the attention of scientists. The luminescence properties of RE^{3+} ions exhibit distinct spectral features in solid-state materials, owing to the various possible transitions between 4*fn* energy levels. Notably, Dy^{3+}, Sm^{3+}, and Tb^{3+} ions are extensively studied rare earth metals. It is well-established that materials doped with these RE^{3+} ions emit light in the red, yellow, and green regions of the spectrum, making them widely employed in applications such as fluorescent lamps, field emission displays, plasma display panels, scintillators, cathode ray tubes, and lasers [1]. Aluminum borates have been the subject of extensive research due to their diverse crystal lattices. Among these, the $Al_4B_2O_9$ compound has received the most attention. Its crystal structure was first reported by Scholze [2]. Various preparation techniques have been employed to synthesize $Al_4B_2O_9$, including the solid-state reaction [3], wet molten salt method [4], sol-gel method [5], and combustion method [6]. Due to their intriguing physical properties, morphological structures, and non-toxic nature, aluminum borates find wide-ranging applications in fields such as mechanics, electronics, and optics [4, 7]. Particularly, their optical properties have yielded interesting findings – for instance, the luminescence properties of $Al_4B_2O_9$ doped with Eu^{2+} and Eu^{3+} have been ex-

tensively investigated [3, 6]. However, the photoluminescence (PL) properties of $Al_4B_2O_9:Dy^{3+}$, $Al_4B_2O_9:Sm^{3+}$, and $Al_4B_2O_9:Tb^{3+}$ have not been studied thus far.

This paper addresses the preparation of RE^{3+} ions (Dy^{3+}, Sm^{3+}, and Tb^{3+})-activated $Al_4B_2O_9$ materials by the solution combustion method. The synthesized aluminum borates were characterized using powder XRD, and the PL properties of RE^{3+}-activated aluminum borates were investigated in detail at room temperature.

Experimental. The solution combustion method was used to prepare RE^{3+} ions (Dy^{3+}, Sm^{3+}, and Tb^{3+})-activated $Al_4B_2O_9$ powders. In the synthesis stage, the raw chemicals are $Al(NO_3)_3 \cdot 9H_2O$ (Sigma-Aldrich ≥99%), H_3BO_3 (Merck ≥99.8%), and $(NH_2)CO(NH_2)$ (Merck ≥99%). Additionally, $Dy(NO_3)_3 \cdot 5H_2O$ (Alfa Aesar ≥99.9%), $Sm(NO_3)_3 \cdot 6H_2O$ (Sigma-Aldrich ≥99.9%) and $Tb(NO_3)_3 \cdot 5H_2O$ (Sigma-Aldrich ≥99.9%) were also used as the activator chemicals. In an analytical balance, the appropriate amounts of $Al(NO_3)_3 \cdot 9H_2O$, H_3BO_3, $(NH_2)CO(NH_2)$, and activator materials were weighted separately. The precursor powders were then combined in a beaker and dissolved in distilled water. Subsequently, the precursor powders were combined in a beaker and dissolved in distilled water. The resulting mixture was then transferred into a porcelain container. These containers were subsequently placed in a furnace and heated at 500ºC for 30 min. Afterward, the containers were removed from the furnace, mixed, and milled. Finally, the precursor powders were carefully placed into an alumina boat and slowly heated at 850ºC in an air-cooled Naberthem furnace for 6 h. The phase and photoluminescence analyses of RE^{3+} activated aluminum borates were conducted using an X-ray Bruker AXS D8 Advance and a Thermo Scientific Lumina fluorescence spectrometer, respectively.

Results and discussion. *X-ray powder diffraction analysis.* $Al_4B_2O_9$ has been identified as having orthorhombic unit cells, with dimensions of a = 14.7460 Å, b = 15.2680 Å, c = 5.5570 Å, and a Z value of 8 [2]. Figure 1 illustrates the XRD pattern of $Al_4B_2O_9:Dy^{3+}$, $Al_4B_2O_9:Sm^{3+}$, and $Al_4B_2O_9:Tb^{3+}$. The relative intensities and positions of all diffraction peaks were found to be consistent with the PDF Card No: 00-029-0010. The structures of the synthesized aluminum borates exhibited conformity with those of $Al_4B_2O_9$, and the doping of RE^{3+} ions did not substantially affect the crystal structure of $Al_4B_2O_9$.

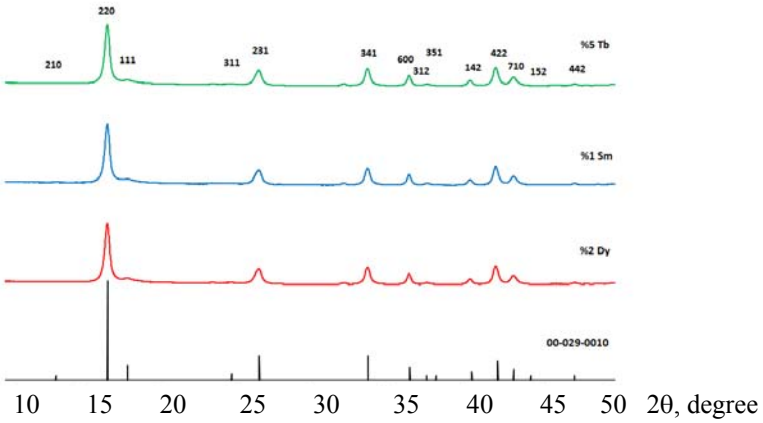

Fig. 1. XRD pattern obtained for $Al_4B_2O_9:Dy^{3+}$(2%), $Al_4B_2O_9:Sm^{3+}$(1%), and $Al_4B_2O_9:Tb^{3+}$(5%) prepared by a solution combustion method.

Photoluminescence of $Al_4B_2O_9:Dy^{3+}$. Dy^{3+} ions exhibit complex $4f^9$ energy levels, leading to the presence of selective and distinct peaks in the spectra attributed to various possible transitions [8, 9]. The excitation spectrum of $Al_4B_2O_9:Dy^{3+}$ (2%) was obtained with emission at 578 nm (Fig. 2a). The spectrum displays six peaks arising from both *f–d* and *f–f* transitions of Dy^{3+}. The peak observed at 298 nm is attributed to the forbidden *f–d* transition [10, 11]. Additionally, there are five excitation peaks between 300 and 450 nm arising from 4*f*–4*f* transitions. These peaks at 326, 352, 366, 389, and 426 nm, respectively, have been assigned to the transitions from $^6H_{15/2}$ to $^4L_{19/2}$, $^6P_{7/2}$, $^6P_{5/2}$, $^4I_{13/2}$, $^4G_{11/2}$ of Dy^{3+} [12, 13]. The emission spectrum of $Al_4B_2O_9:Dy^{3+}$ (2%) was measured upon excitation at 352 nm (Fig. 2b). The spectrum has two major peaks at 484 and 578 nm, which are assigned to the transitions $^4F_{9/2}\rightarrow{}^6H_{15/2}$ and $^4F_{9/2}\rightarrow{}^6H_{13/2}$, respectively. The transition of $^4F_{9/2}\rightarrow{}^6H_{11/2}$ is observed as a weaker peak at 701 nm [14].

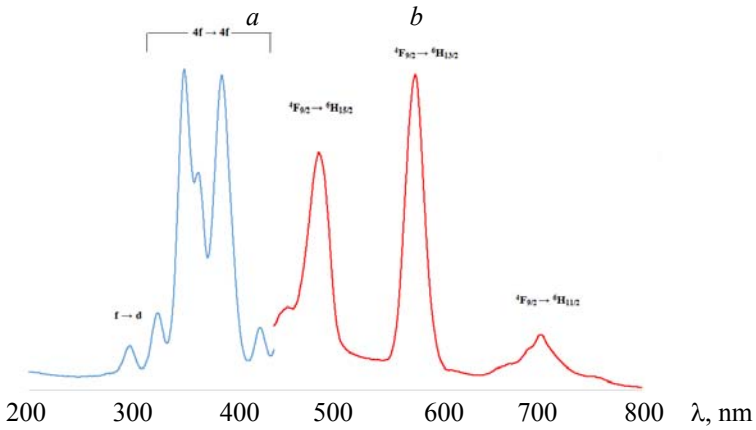

Fig. 2. The excitation (a) and emission (b) spectra of $Al_4B_2O_9:Dy^{3+}$(2%) at room temperature (λ_{exc}= 352 nm, λ_{em}= 578 nm).

Photoluminescence of $Al_4B_2O_9:Sm^{3+}$. Due to the various potential transitions between the 4*f*-levels, it has been observed that materials doped with Sm^{3+} exhibit a broad range of peaks. These transitions enable the emission characteristics of the materials to span from the orange to the near-infrared regions of the spectrum [15, 16]. The excitation spectrum of $Al_4B_2O_9:Sm^{3+}$ (1%) was measured upon emission at 599 nm (Fig. 3a). The spectrum contains seven peaks, depending on the 4*f*–4*f* transitions of Sm^{3+}. The peaks at 345, 362, 375, 402, 417, 440, and 470 nm have been assigned to the transition from $^6H_{5/2}$ to $^4H_{9/2}$, $^4D_{3/2}$, $^6P_{7/2}$, $^6L_{13/2}$, $^6P_{5/2}$, $^4G_{9/2}$, and $^4I_{13/2}$ of Sm^{3+}, respectively [14, 17–20]. The emission spectrum of $Al_4B_2O_9:Sm^{3+}$(1%) was measured upon excitation at 402 nm (Fig. 3b). The spectrum has three major peaks at 563, 599, and 645 nm, which are assigned to the transitions $^4G_{5/2}\rightarrow{}^6H_{5/2}$, $^4G_{5/2}\rightarrow{}^6H_{7/2}$, and $^4G_{5/2}\rightarrow{}^6H_{9/2}$, respectively. Also, the transition of $^4G_{5/2}\rightarrow{}^6H_{11/2}$ is observed as a weaker peak at 702 nm [14, 15, 21].

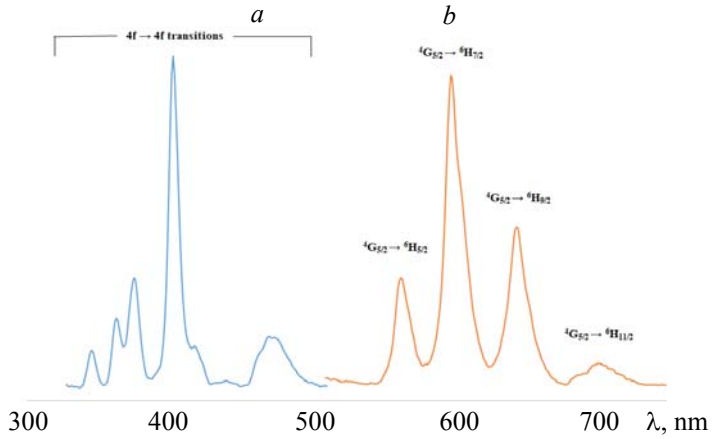

Fig. 3. The excitation (a) and emission (b) spectra of $Al_4B_2O_9:Sm^{3+}$(1%) at room temperature (λ_{exc}= 402 nm, λ_{em}= 599 nm).

Photoluminescence of $Al_4B_2O_9:Tb^{3+}$. The electronic configuration of trivalent terbium (Tb^{3+}) is $4f^8$, which leads to the emission of green light resulting from the transition $^5D_4\rightarrow{}^7F_5$ [22]. The excitation spectrum of $Al_4B_2O_9:Tb^{3+}$(5%) was measured with emission at 544 nm (Fig. 4a). The spectrum exhibits numerous peaks, corresponding to the 4*f*–4*f*5*d* and 4*f*–4*f* transitions of Tb^{3+}. The broad band between 200 and 300 nm is attributed to the $4f^8\rightarrow4f^75d^1$ transition of Tb^{3+} caused by dipolar electric parity allowed transitions [23]. Additionally, a few peaks between 300 and 400 nm can be ascribed to the 4*f*→4*f* transitions of Tb^{3+}. Specifically, these peaks at 304, 318, 341, 352, 370, and 378 nm are assigned to the transitions from $^7F_6$ to $^3H_6$, $^5D_0$, $^5L_7$, $^5L_9$, $^5G_5$, and $^5D_3$ of Tb^{3+} [22, 25]. The emission spectrum of $Al_4B_2O_9:Tb^{3+}$(5%) was obtained by exciting at 238 nm (Fig. 4b). The spectrum exhibits four prominent peaks at 489, 544, 588, and 622 nm, corresponding to the transitions $^5D_4\rightarrow{}^7F_6$, $^5D_4\rightarrow{}^7F_5$, $^5D_4\rightarrow{}^7F_4$, and $^5D_4\rightarrow{}^7F_3$, respectively. Among these peaks, the transition $^5D_4\rightarrow{}^7F_5$ is observed as the strongest peak at 544 nm [20–22, 24, 25].

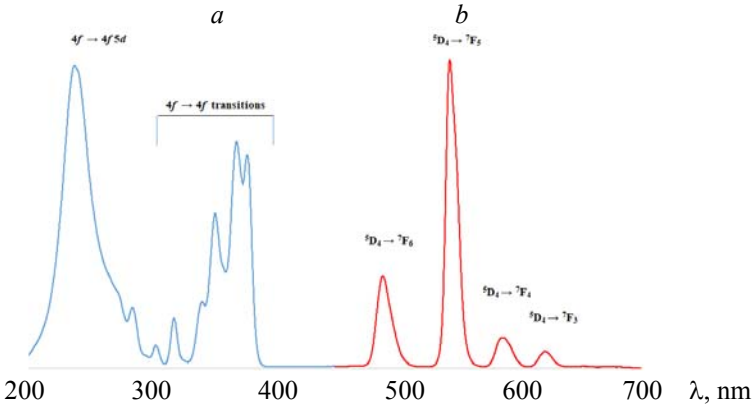

Fig. 4. The excitation (a) and emission (b) spectra of $Al_4B_2O_9:Tb^{3+}$(5%) at room temperature (λ_{exc}= 238 nm, λ_{em}= 544 nm).

Conclusions. The solution combustion method was utilized to synthesize three novel phosphors: $Al_4B_2O_9:Dy^{3+}$, $Al_4B_2O_9:Sm^{3+}$, and $Al_4B_2O_9:Tb^{3+}$. The photoluminescence properties of these phosphors were comprehensively investigated using a fluorescence spectrometer. Under excitation at 352 nm, $Al_4B_2O_9:Dy^{3+}$ emitted light at 484, 578, and 701 nm. Similarly, $Al_4B_2O_9:Sm^{3+}$, when excited at 402 nm, exhibited emission peaks at 563, 599, 645, and 702 nm. Lastly, $Al_4B_2O_9:Tb^{3+}$, upon excitation at 238 nm, emitted light at 489, 544, 588, and 622 nm. Thus, all three synthesized materials demonstrated radiation emission in the visible region. Consequently, these novel phosphors hold promise for applications in visible LED development.

REFERENCES

1. J. Garćıa Solé, L. E. Bausá, D. Jaque, *An Introduction to the Optical Spectroscopy of Inorganic Solids,* Wiley, 199 (2005).
2. H. Scholze, *Z. Anorg. Allgem. Chem*., **284**, 272–277 (1956).
3. Y. Zheng, D. Chen, *Luminescence*, **26**, 481–485 (2011).
4. X. Zhang, Z. Liu, Y. Zhou, J. Yu, *Ceramics-Silikáty*, **62**, 81–85 (2018).
5. Y. Fan, et al., *J. Nanopart. Res*., **15**, 1699 (2013).
6. A. N. Yerpude, S. K. Ramteke, G. N. Nikhare, V. R. Panse, N. S. Kokode, S. J. Dhoble, *Mater. Today: Proc.*, **29**, 857–860 (2020).
7. Y. Dong, et al., *Ceram. Inter*., **47**, 21029–21037 (2021).
8. I. M. Nagpure, K. N. Shinde, S. J. Dhoble, A. Kumar, *J. Alloys Compd*., **481**, 632–638 (2009).
9. H. Choi, Ch. H. Kim, Ch. H. Pyun, S. J. Kim, *J. Lumin*., **82**, 25–32 (1999).
10. P. Dorenbos, *J. Lumin.*, **91**, 91–106 (2000).
11. P. Dorenbos, *J. Lumin.*, **91**, 155–176 (2000).
12. Y. Liu, Z. Yang, Q. Yu, X. Li, Y. Yang, P. Li, *Mater. Lett.*, **65**, 1956–1958 (2011).
13. İ. Pekgözlü, *J. Appl. Spectrosc*., **89**, 799–802 (2022).
14. İ. Pekgözlü, S. Çakar, *J. Lumin*., **132**, 2312–2317 (2012).
15. İ. Pekgözlü, *Optik*, **127**, 4114–4117 (2016).
16. G. E. Malashkevich, I. M. Mel'nichenko, *Phys. Solid State*, **40**, 420–426 (1998).
17. Y. Zhang, C. Lu, L. Sun, Z. Xu, Y. Ni, *Mater. Res. Bull.*, **44**, 179–183 (2009).
18. C. M. Reddy, G. R. Dillip, K. Mallikarjuna, S. Z. A. Ahamed, B. S. Reddy, B. P. Raju, *J. Lumin*., **131**, 1368–1375 (2011).
19. K. Annapurna, R. N. Dwivedi, P. Kundu, S. Buddhudu, *Mater. Res. Bull.*, **38**, 429–436 (2003).
20. E. Cavalli, A. Belletti, R. Mahiou, P. Boutinaud, *J. Lumin.*, **130**, 733–736 (2010).
21. İ. Pekgözlü, H. Karabulut, A. Mergen, A. S. Başak, *J. Appl. Spectrosc*., **83**, 504–511 (2016).
22. E. Erdoğmuş, İ. Pekgözlü, C. Özpınar, E. Korkmaz, *J. Appl. Spectrosc*., **81**, 313–316 (2014).
23. T. Kano, S. Shionoya, W. M. Yen, *Phosphor Handbook*, CRC Press, Boca Raton, 185 (1998).
24. P. Li, Z. Wang, Z. Yang, Q. Guo, X. Li, *J. Lumin.*, **130**, 222–225 (2010).
25. R. Wang, J. Xu, C. Chen, *Mater. Lett.*, **68**, 307–309 (2012).